DEFICIENCY OF GROWTH HORMONE SECRETAGOGUE RECEPTOR IN MYELOID CELLS ATTENUATE THE NEUROINFLAMMATION OF CLP-INDUCED SEPSIS

A Thesis

by

PENGFEI JI

Submitted to the Graduate and Professional School of
Texas A&M University
in partial fulfillment of the requirements for the degree of

MASTER OF SCIENCE

Chair of Committee,	Yuxiang Sun
Committee Members,	Gus A. Wright
	Jianrong Li
	Jiang Chang
Head of Department,	David W. Threadgill

December 2021

Major Subject: Nutrition

ABSTRACT

Sepsis is a threat to human healthy and caused by infection with a systemic inflammatory response. Sepsis ranges from endotoxemia to more severe and long-term effects. Moreover, the low blood pressure and inflammation patients experience during sepsis may lead to brain damage and cause cognitive problem. Growth hormone secretagogue receptor (GHS-R) is recognized as ghrelin receptor which is a G-protein coupled receptor. We previously reported that mice with global GHS-R ablation plays important roles in macrophage polarization during aging and diet induced inflammation. Thus, we created *LysM-Cre;Ghsr*$^{flox/flox}$ mice to determine the role of GHS-R in myeloid cells. Remarkably, we detected that deletion of GHS-R in myeloid cells ameliorates neuroinflammation and protects brain from septic shock-induced behavioral impairments. Obviously, we found that significantly decreasing of M1-like macrophages and increasing of M2-like macrophages in the brain of these septic mice, consistently found reduced expression of pro-inflammation cytokines. In conclusion, our data indicated that GHS-R ablation in myeloid cells protects against sepsis, improve survival ratio, and mitigating the brain inflammation. In this project, I aim to reveal the pathobiology of sepsis and whether GHS-R can be a treatment strategy for sepsis-induced neuroinflammation.

DEDICATION

I dedicate this thesis to my family and many friends. Especially, many thanks to my lab member Yan Liu, who has fully supported and encouraged me to study during the challenges of my life and research. People say that parents are the teachers. I couldn't agree more. This work is also dedicated to my parents, Andong Ji and Lixia Sun. My parents were both in academics and pharmaceutical developments for long years. Their dedication to this field since my childhood has greatly inspired my desire for gaining biological knowledge.

ACKNOWLEDGEMENTS

I would like to thank my committee chair, Dr. Yuxiang Sun, for fully supporting me and bringing big help in this project. Her big help has guided me better throughout the course of this research.

Also, thanks to my committee members Dr. Gus A. Wright, Dr. Jianrong Li and Dr. Jiang Chang for improving my knowledge and skills. Their suggestions and advice always guide me and improve my critical thinking in this project

I would also like to thank Yan Liu for teaching me on the experiment skills and data sharing. Additionally, she taught me how to use different software to analyze the data. Thanks to her experience and knowledge of this project.

Finally, thanks to the other lab members and my parents for their help and encouragement.

CONTRIBUTORS AND FUNDING SOURCES

Contributors

This work was supervised by a thesis committee consisting of Dr. Yuxiang Sun and Dr. Gus A. Wright of the Department of Nutrition and Dr. Jianrong Li and Dr. Chang Jiang of the Department of Veterinary Medicine.

We greatly appreciate the excellent technical assistance of Dr Gus A. Wright in the Flow Cytometry Facility at Texas A&M University. Also, very thanks to Yan Liu for helping and cooperating for my project thesis and teaching of the experiment skills.

The data analyzed for Chapter 3 was provided by Yan Liu including the survival curves, multiplex plate, and western blot.

All other work conducted for the thesis was completed by the student independently.

Funding Sources

Graduate study was supported by a fellowship from Texas A&M University and a dissertation research fellowship from Foundation.

This work was made possible in part by the support of NIH R01DK118334, NIH AG064869, and BrightFocus Foundation A2019630S to Dr. Yuxiang Sun. This work was also supported in part by the USDA Hatch project 1010840 and Multistate project NE1939 (Dr. Yuxiang Sun).

NOMENCLATURE

GHS-R	Growth Hormone Secretagogue Receptor
CNS	Central Nervous System
CLP	Cecal Ligation Puncture
LPS	Lipopolysaccharide
BBB	Brain Blood Barrier
OPT	Open Field Test
TST	Tail Suspension Test
qPCR	Quantitative real-time Polymerase Chain Reaction
WB	Western Blot
TNF-α	Tumor Necrosis Factor-alpha
IL-1β	Interleukin 1 beta
IL-6	Interleukin 6
MCP1	Monocyte Chemoattractant Protein 1
BDNF	Brain Derived Neurotrophic Factor
IRS2	Insulin Receptor Substrate 2
PI3K	Phosphoinositide 3-kinase
AKT	Protein Kinase B
mTOR	Mammalian Target of Rapamycin
NF-κB	Nuclear Factor Kappa B
NLRP3	NLR family pyrin domain containing 3
MAPK	Mitogen-activated Protein Kinase

PBS	Phosphate-Buffered Saline
BMDM	Bone Marrow Derived Macrophage

TABLE OF CONTENTS

Page

ABSTRACT ii

DEDICATION iii

ACKNOWLEDGEMENTS iv

CONTRIBUTORS AND FUNDING SOURCES v

NOMENCLATURE vii

TABLE OF CONTENTS viii

LIST OF FIGURES xii

LIST OF TABLES xiv

INTRODUCTION 1

MATERIALS AND METHODS 2

- Animals 2
- Cecal Ligation and Puncture 2
- Assessment of mortality rate 3
- MILLIPLEX Multiplex Assays 3
- Quantitative real-time PCR 4
- Open field test 5
- Tail Suspension test 6
- Flow cytometry 6
- Immunofluorescence 7
- Western Blot 7
- Statistical analysis 8

RESULTS AND DISCUSSIONS 9

- Ablation of GHS-R in myeloid cells improve the survival ratio of CLP-associated sepsis and attenuate inflammation 9
- Deletion of myeloid-specific GHS-R can protect mice from the stress, pressure, and anxiety of CLP-induced sepsis 9
- Ablation of myeloid-specific GHS-R does not modulate the microglia migration in cortex and hippocampus under CLP treatment 11

Deletion of GHS-R in myeloid cells reduce neuroinflammation in various brain regions under CLP treatment 12
Suppression of myeloid-specific GHS-R mediated the infiltration of macrophage in brain under CLP-induced sepsis 15
Suppression of myeloid-specific GHS-R promote macrophage polarization through IRS2/PI3K/AKT/mTOR and NF-κB cell signaling pathways 16

CONCLUSION 19

REFERENCES 30

LIST OF FIGURES

Page

Figure 1 Survival curve and inflammatory cytokines in serum 20

Figure 2 Open field test and tail suspension test 21

Figure 3 Immunofluorescence 22

Figure 4 Pro-inflammatory cytokines and BDNF 24

Figure 5 Flow cytometry 26

Figure 6 Western Blot of cell signaling pathway 27

Figure 7 Potential cell pathway 28

LIST OF TABLES

TABLE Page

1 Sequence of primers used in the qPCR analysis 29

2 Antibodies used to stain cells 29

INTRODUCTION

Ghrelin is known as “hungry hormone”, and it is a 28 amino acid peptide hormone secreted by the stomach and related with glucose homeostasis and cognition[1]. Also, one of its functions is to serve as a neuropeptide in the central neural system (CNS)[2]. Currently, it is unknown how Ghrelin plays important roles and works in the brain[3].Yet, ghrelin can go through the blood brain barrier and bind to ghrelin receptors in the brain[4]. Growth hormone secretagogue receptor (GHS-R) is recognized as the ghrelin receptor and is also found in the brain. Our published studies have revealed that ablation of GHS-R plays an important metabolic role in impairing insulin resistance and protecting against age-associated obesity and inflammation[5]. Additionally, several studies highlight the negative correlation between ghrelin levels and both IR and body weight[6]. Also, GHS-R is a G-couple protein receptor and highly expressed in brain and mature macrophages, but its expression is extremely low in other peripheral tissues [7]. Intriguingly, it is found that GHS-R is extremely high expressed in the hypothalamus, particularly the ventromedial nucleus and arcuate nucleus, GHS-R is also expressed in the hippocampus, ventral tegmental area in the brain[8]. In addition, our previous data revealed that deficits of GHS-R play important roles in anti-aging and regulation of glucose homeostasis and reduce proinflammatory cytokines[5]. Indeed, the previous study found that global GHS-R knockout mice would not have influences and effects on impair the growth[9]. Furthermore, high-fat diet induced inflammation showed that deficiency of GHS-R improved anti-inflammatory macrophage polarization[10]. Therefore, GHS-R can be a potential marker in the brain.

Sepsis is a life-threatening disease and severe inflammatory condition caused by infection and system immune response triggered by bacteria, fungi, or virus. Sepsis commonly displays a range of symptoms ranging from endotoxemia to septic shock, from acute to chronic effects[11]. In addition, sepsis has several symptoms including fever, confusion, dramatic fluctuation in body temperature and heart failure, which can lead to high death rate[12]. Patients during sepsis suffer potential brain damage, which can lead to cognitive impairment, especially delirium symptoms; a state known to be associated with Alzheimer's disease[13]. Indeed, there are no molecular ways to diagnose sepsis, and also there is no specific targeted therapy for sepsis mediators[14].

In this study, we generate the myeloid-specific GHS-R knockout mice to understand the pathobiology of sepsis. The cecal ligation and puncture (CLP) surgery is mostly used in experimental models of sepsis[15]. Additionally, injection of high dose and concentration of lipopolysaccharide (LPS) can also induce sepsis in mouse models[16]. Several studies indicated that glia cells play important roles during brain inflammation[17]. Alternatively, peripheral macrophages infiltrated into the CNS through BBB caused by the inflammation and damages of sepsis. Thus, myeloid cells can be infiltrated into the CNS under sepsis-induced brain inflammation. In this project, I aim to reveal the pathobiology of sepsis and whether GHS-R can be a marked therapy strategy for sepsis-associated neuroinflammation.

MATERIALS AND METHODS

Animals

Our published papers indicated the GHS-R floxed mice were acquired from the Taconic Farms[18, 19]. As our published paper stated, we used Lysozymes-Cre (*LysM-cre*) [33] mice breeding with $Ghsr^{f/f}$ to obtain the *LysM-cre;* $Ghsr^{f/f}$. Age matched male $Ghsr^{f/f}$ and *LysM-cre;* $Ghsr^{f/f}$ mice were fed with a regular diet (RD) from Harlan Teklad 2920X (Madison, WI, USA). Mice were in the animal facility of Texas A&M University (college station, Texas) with on 12 hours light and 12 hours dark cycles (lights on at 6:00 AM) at 75^{o} F ± 1^{o} F. The composition of regular diet (RD) 2920X (Madison, WI, USA) with the caloric composition of 16% from fat, 60% from carbohydrates, 24% from protein. All experimental protocols were approved by the institutional animal care and use committee of Texas A&M University (College station, Texas).

Cecal ligation and puncture

Cecal ligation and puncture (CLP) procedures to induce sepsis in the mice. In this surgical procedure, mice were anesthetized and maintained with isoflurane (1-5% with 95-99% Oxygen). Sterile ophthalmic ointment was placed in the eyes after animals become unconscious to prevent corneal drying. Then, avoid the exposure of eyes to surgical scrub solutions. The ventral abdomen was devoid of hair by shaving. Then, the surgical site was scrubbed with povidone iodine three times followed by 70% ethanol scrubs three times. Open the abdominal cavity with

about 1cm long cut on the abdominal wall. Then pull out the cecum and ligate the distal portion of the ileocecal valve with 4-0 silk suture making sure to not disrupt bowel continuity. The cecum was then punctured twice using an 18 Gauge needle and a small amount of feces were forced to extrude into the abdominal cavity to ensure infection patency of the puncture before returning it back to the abdominal cavity. Sham operated animals were also undergoing an identical surgical procedure including laparotomy and cecal isolation but without cecal puncture. The abdominal wall was then closed with 4-0 silk suture. Post-operation, the mice were given warmed saline (50 ml/kg) subcutaneously to prevent dehydration.

Assessment of mortality rate

Survival ratio studies were conducted to determine whether GHS-R deletion in myeloid cells could reduce the mortality in CLP-induced sepsis mice. Mice (sham n=14, *CLP-Ghsr*$^{f/f}$ n=18, *CLP-LysM-cre; Ghsr*$^{f/f}$ n=14) were monitored every two hours on the first day, then twice a day up to 7 days.

MILLIPLEX Multiplex Assays

The blood was collected from the mice which were euthanized 24 hours after CLP or sham surgery. Then, the blood was centrifuged at 300×g for 5 minutes at 4 ℃ and transferred to the supernatant to get the serum. To assess the cytokines in the serum, we used the MILLIPLEX® Multiplex Assays Using Luminex® (Milipore, USA) kits. Assays were loaded as

the manufacturers' instructions with duplication of samples and incubated the samples overnight with shaking at 4 ℃. Additionally, utilize the magnetic block for following steps.

Quantitative real-time PCR

Total RNA was extracted by using Aurum™ Total RNA Mini Kit (*Bio-Rad*). After that, the cDNA was synthesized from the total RNA using Script™ Reverse Transcription Supermix (Bio-Rad). Then, utilized the SsoAdvanced™ Universal SYBR® Green Supermix (*Bio-Rad*) to do quantitative real-time PCR in duplicates on CFX384 Touch™ Real-Time PCR Detection System (*Bio-Rad*). Relative mRNA expression levels were normalized by housekeeping gene cyclophilin. The Ghsr1a primers used were as follows: forward primer 5'-GGACCAGAACCACAAACAGACA-3' and reverse primer 5'-CAGCAGAGGATGAAAGCAAACA-3'[20]. The rest of the primer information is provided in Table 1.

Open field test

Open field test was performed as the published paper method[21]. We used the multiple unit open field maze (OFM) and the chamber is 50 cm length x 50 cm width x 38 cm height. Put the mice in the chamber for 30 minutes. The Ethovision XT Tracking software can track the mouse movement and record. Wipe the chamber with ethanol before using the chamber to avoid the odour influence. The Ethovision XT system in the Rodent Preclinical Phenotyping Core in Texas A&M

University was used to monitor open field activity. The travel distance, and time spent in the inner zone, fecal boil count was analyzed.

Tail suspension test

Tail suspension test is a mouse behavior test to assess depression and stress level [22]. It is performed in the dimensions (55 height X 60 width X 11.5 cm depth). Using the camera to record the animals' behavior, the tape is used within 2-3 cm at the end of tails to avoid the animal's climbing. The camera records from start to finish for 6 minutes for each mouse.

Flow cytometry

Collect brain tissues with cutting to small pieces and digest these tissues by using StemPro Accutase in the 15mL tubes. Pipette up and down to mix up the tissues and incubate for 30 minutes. Transfer the mixture to the 50 mL tubes and with a 70 um filter. Then, add 50% percoll and 70% percoll with PBS to the 15 mL tube. Then, centrifuge the tube with 2000g for 20 mins at 17 ℃, and gently remove and transfer the interface liquid to intracellular flow tubes[23]. Cells were stained with Live/dead aqua for 30 mins at 4 ℃, and 1x10 6 cells/100 uL of FC block in PBS for 10 min at 4 ℃. After that, prepare the "cocktail" mix with CD45-APC, CD11b-APC-cy7, Tmem119-AF488, Ly6G-PE, F4/80-Pe-cy7, CD206-eFluor450 and CD86-BB700 Table 2. The concentration of the cocktails is in table 2 below. Flow Cytometric data were obtained by using MoFlo Astrios Cell Sorter (Beckman Coulter, USA) and analyzed by using FlowJo 10.0 software (BD, USA). All cells were gated based on forward (FSC-A) and side (SSC-A) scatters)

to exclude cell debris. Then, singlets were further gated using FSC-A versus FSC-H plotting. Dead cells were excluded with the live/dead fixable aqua marker (Invitrogen, USA)[24-26].

Immunofluorescence

Mice were anesthetized with isoflurane. The brains were stored and fixed with 10% formalin for 24 hours. Then, the brains were transferred and dehydrated by immersion in 15% sucrose in PBS, later 30% sucrose in PBS at 4 ℃. The brains were embedded by OCT and 20 um frozen sections were cut by using a slider (LEICA CM1950). Staining was performed on floating sections. The slices were staining with antibody (anti-Iba1, Wako, 019-19741) at 1:500 dilution, and put the slices on the super frosted glass slides and cover the slides with Mounting Shield including DAPI (Vector Laboratories, Burlingame, CA, USA). Images were taken with a Leica confocal microscope (LEICA TCS SPE).

Western Blot

Cell pellets from bone marrow were digested with RIPA buffer including Complete Protease Inhibitor Cocktail (cOmplete™ ULTRA Tablets, Mini, EDTA-free, EASYpack Protease Inhibitor Cocktail, Roche) and PhosSTOP phosphatase inhibitor cocktail (PhosSTOP™, PHOSS-RO, Roche). The protein concentration was measured by BSA protein assay kit (Lot # NH17739, Thermo, Pierce).

Dilute and mix the amounts of protein to the volume (20-40ug) were loaded on the 8-10% sodium dodecyl sulfate-polyacrylamide electrophoresis gels (8-10% SDS-PAGE), and then

put the gel onto NF membranes (Milipore Corp). The membranes were subsequently blocked with 10% BSA 1 hour at room temperature, then put the membrane with the primary antibodies overnight at 4℃ over night (the primary antibodies would be diluted according to the manufactures' instructions). Then, the membranes were transferred into the secondary antibody solution (1:3000, CST, USA) for 1 hour at room temperature.

Statistical analysis

Analysis data by using Unpaired two-tailed t-test and Two-way ANOVA or one-way ANOVA with Tukey's post hoc test. Also, data were presented as mean ± SEM and P value less than. 0.05 was a significant statistical difference. All data details have been shown at the figure legends.

RESULTS AND DISCUSSIONS

Ablation of GHS-R in myeloid cells improves the survival ratio of CLP-associated sepsis and attenuates inflammation.

In the CLP-induced sepsis group, the survival rate markedly increased in the *LyM-cre;Ghsr*$^{f/f}$ compared with wild type (*Ghsr*$^{f/f}$) group ($p<0.01$) (**Fig.1A**). However, there are no significant differences between *Ghsr*$^{f/f}$ and *LyM-cre;Ghsr*$^{f/f}$ in the sham control group, which means that myeloid cells specific GHS-R knockout mice are not being influenced under normal conditions compared with wild type mice. After CLP-induced inflammation, mice have different rates of mortality. To be more specific, *LyM-cre;Ghsr*$^{f/f}$ mice can resist inflammation more effectively than wild type mice. Furthermore, we detect the pro-inflammatory cytokines in the serum including TNF-α and IL-1β, and found that TNF-α and IL-1β both are significantly decreasing in *LyM-cre;Ghsr*$^{f/f}$ mice compared to *Ghsr*$^{f/f}$ mice under CLP treatment ($p<0.01$) (**Fig. 1B**). Therefore, it indicated that *LyM-cre;Ghsr*$^{f/f}$ mice have less inflammation than wild type after CLP-induced sepsis.

Deletion of myeloid-specific GHS-R can protect mice from the stress, pressure, and anxiety of CLP-induced sepsis.

To further detect the brain function whether affected by deletion of myeloid cell specific GHS-R knockout after CLP-induced sepsis. (**Fig. 2A**) We did the open field test to test the stress and anxiety of the *LysM-cre;Ghsr*$^{f/f}$ mice after mice treat with CLP surgery at day3, and found

that the *LysM-cre;Ghsr*$^{f/f}$ mice have significantly increased the total distance movement comparing with *Ghsr*$^{f/f}$ mice group ($p<0.05$), which means that *LysM-cre;Ghsr*$^{f/f}$ mice have more exploratory activity and less pressure and anxiety. Locomotor activity of the test subjects plays important roles in analysis of OFT, and locomotor ability consists of the therapy influences and drug treatments[21]. Moreover, *LysM-cre;Ghsr*$^{f/f}$ mice have more mobile times than *Ghsr*$^{f/f}$ mice under CLP treatment showing more vulnerable mobility ($p<0.05$). Furthermore, we detect that the *LysM-cre;Ghsr*$^{f/f}$ mice have more movement times in the inner zone than the *Ghsr*$^{f/f}$ mice, and these results indicated that *LysM-cre;Ghsr*$^{f/f}$ mice has less thigmotaxis than wild type mice under CLP treatment. Thigmotaxis is the method to assess and evaluate the mice anxiety level, and thigmotaxis or wall-hugging behavior is associated with anxiety or pressure-related behavior[27, 28].

Moreover, to investigate the depression and stress level of the mice after CLP surgery treatment. We process the tail suspension test to measure the stress and depression in the septic mice model after CLP treatment at day5. The experiment method is to observe the mice immobile time and mobile time on the short-time and inescapable stress of tail suspension. Indeed, the force swimming test is another option to test the depression and stress, however, the mice were under CLP surgery, and it is very weak to keep in touch with the water[29]. Therefore, we choose a tail suspension test to improve the quality of data. Each mouse was tested and recorded for 6 minutes[30], and we used a camera to monitor the mouse in order to eliminate the man-made-interference. (**Fig. 2B**) The data showed that the sham control groups are no different between the *Ghsr*$^{f/f}$ mice and the *LysM-cre;Ghsr*$^{f/f}$ mice. In addition, we found that the CLP groups have significantly difference between the *Ghsr*$^{f/f}$ mice and the *LysM-cre;Ghsr*$^{f/f}$

mice. Specifically, the mobile time of the *LysM-cre;Ghsr$^{f/f}$* mice has improved a lot compared with the *Ghsr$^{f/f}$* mice in the record 6 minutes. Also, the immobile time of the *LysM-cre;Ghsr$^{f/f}$* mice was reduced compared with the *Ghsr$^{f/f}$* mice. Therefore, the myeloid cell specific GHS-R knockout mice have reduced the depression and stress compared with the wild type mice.

Ablation of myeloid-specific GHS-R does not modulate the microglia migration in cortex and hippocampus under CLP treatment

Microglia are the resident macrophage, and it is the first act immune cell to protect the central nervous system (CNS)[31]. The immunostaining is the experimental method to label the microglia and other cells migration. Allograft inflammatory factor 1 is a protein also named IBA1[32], and IBA1 can combine and label with the microglia. Therefore, we choose IBA1 to label microglia with FITC fluorescence, which luminate green color[33]. Additionally, we evaluate the non-microglia myeloid cells by td-TOMATO expression in *LysM-Cre; Rosa26-tdTOMATO*; *Ghsr$^{f/f}$* mice and *Rosa26-tdTOMATO*; *Ghsr$^{f/f}$* mice, and TdTomato is an extremely bright red fluorescence[34]. Furthermore, DAPI is widely used to identify and stain the cell nucleus[35], and DAPI showed strong blue color. To further detect the microglia migration in the brain of the CLP treatment mice, we did immunofluorescence with staining TdTomato, IBA1 and DAPI antibodies in cortex and hippocampus slides. (**Fig. 3A & 3B**) Furthermore, there are also no differences between *LysM-Cre; Rosa26-tdTOMATO*; *Ghsr$^{f/f}$* mice and *Rosa26-tdTOMATO*; *Ghsr$^{f/f}$* mice in the CLP treatment groups. Additionally, some papers indicated that *LysM-Cre* mice can mediate recombination with neurons in brain[36]. However, we did not find any different between *LysM-Cre*; *Ghsr$^{f/f}$* mice and *Ghsr$^{f/f}$* mice with the Td Tomato and IBA1. In

that case, the neurons and microglia did not play important roles in septic mouse model. In the OFT and TST behavior test, we have gotten the significantly different data between *LysM-Cre*; *Ghsr*$^{f/f}$ mice and *Ghsr*$^{f/f}$ mice. Thus, it indicated that the infiltrated myeloid cells may play important roles in the septic mouse model. In summary, the microglia do not modulate the neuroinflammation caused by CLP-induced sepsis.

Deletion of GHS-R in myeloid cells reduce neuroinflammation in various brain regions under CLP treatment

LysM-Cre; *Ghsr*$^{f/f}$ mice are the specific myeloid GHS-R knockout mice, and we dissected brain regions including hypothalamus, hippocampus, and cortex. Since we found that the phenotype of the behavior test showed that the *LysM-Cre*; *Ghsr*$^{f/f}$ mice reduce depression, stress, and anxiety. Furthermore, several papers indicated that during the first 3-4 days typical inflammation caused by CLP surgery, and the inflammation gradually decreases after 4 days. Therefore, we choose day 8 as the recovery stage and day 3 as the acute stage of the CLP-induced sepsis[37, 38].

In hypothalamus, we found that the relative RNA expression of pro-inflammatory cytokines is reducing dramatically. (**Fig. 4A**) To be more specific, we found that TNF-α were significantly decreasing in *LysM-Cre*; *Ghsr*$^{f/f}$ compared with *Ghsr*$^{f/f}$ after CLP treatment at day1 and day8 ($p<0.05$). Additionally, we found that the TNF-α expression is higher in day8 than in day1. There are two possible reasons to explain that condition. One explanation is that the inflammation is delayed in the brain and causes the slowly increasing TNF-α expression. The

other explanation is that the experiment of qPCR has some random variation if the cytokines concentration is very low. The TNF-α is also named as Tumor Necrosis factor, and it is a small protein secreted by myeloid cells such as macrophages[39]. Also, the function of TNF-α is to regulate the immune cells and response to the sepsis[40]. Moreover, there are no significant differences between *LysM-Cre*; *Ghsr*$^{f/f}$ and *Ghsr*$^{f/f}$ in sham control groups. Interleukin 1 beta is also known as IL-1β, and a key mediator of the inflammatory response caused by sepsis. It is also important for the host immune response, and it aggravates damages during acute tissue injury[41]. (**Fig. 4B**) Also, we detected the IL-1β relative RNA expression in hypothalamus and found that IL-1β is crucially increased in the *Ghsr*$^{f/f}$ comparing with *LysM-Cre*; *Ghsr*$^{f/f}$ after CLP treatment at day1. Furthermore, interleukin 6 is named IL-6 and it can serve as the crucial mediator during acute stage response of sepsis[42]. Additionally, it has been reported that IL-6 is also related to the pathology of depression, and IL-6 can inhibit the brain-derived neurotrophic factor (BDNF) expression in the brain[43]. (**Fig. 4C**) We found that *LysM-Cre*; *Ghsr*$^{f/f}$ is dramatically decreasing the IL-6 compared with *Ghsr*$^{f/f}$ after CLP treatment at day1. Monocyte chemoattractant protein-1 (MCP1) is the key cytokines that control and regulate the infiltration of macrophages and monocytes[44]. (**Fig. 4D**) Our data indicated that *LysM-Cre*; *Ghsr*$^{f/f}$ has vitally decreased the MCP1 compared with *Ghsr*$^{f/f}$ after CLP-induced sepsis at day1 and day8. As mentioned above, BDNF is an important protein associated with synapse plasticity and also related to learning and memory[45]. Furthermore, it has been reported that the decreasing BDNF is a normal phenotype in the depression of pathology[46]. (**Fig. 4E**) In our study, we did not find any difference between *LysM-Cre*; *Ghsr*$^{f/f}$ and *Ghsr*$^{f/f}$ in hypothalamus.

As the above discussion, we also investigate the deletion of myeloid specific GHS-R whether mediate the function of hippocampus, (**Fig. 4 A, B, C, D&E**) and we found that TNF- α, IL-1β, IL-6 and MCP1 are also significantly reducing at day1 or day8 ($p<0.05$). Surprisingly, the BDNF expression was increasing in *LysM-Cre*; *Ghsr*$^{f/f}$ compared with *Ghsr*$^{f/f}$ at day8 ($p<0.05$). The pro-inflammatory cytokines and BDNF are no different in the sham control groups. The BDNF expression in hippocampus can explain that the behavior test data that the *LysM-Cre*; *Ghsr*$^{f/f}$ mice have decreased the depression, stress, and anxiety comparing with *Ghsr*$^{f/f}$ mice, since BDNF expression is increasing in *LysM-Cre*; *Ghsr*$^{f/f}$ mice. Also, the. Pro-inflammatory cytokines are reduced in the hippocampus of *LysM-Cre*; *Ghsr*$^{f/f}$ mice.

(**Fig. 4 A, B, C, D&E**) In the cortex part, the data showed that proinflammatory cytokines reducing significant in *LysM-Cre*; *Ghsr*$^{f/f}$ comparing with *Ghsr*$^{f/f}$ in CLP groups at day1 or day8, and BDNF expression increased in *LysM-Cre*; *Ghsr*$^{f/f}$ in the CLP-induced sepsis at day8 ($p<0.05$). Moreover, *LysM-Cre*; *Ghsr*$^{f/f}$ decreased in TNF- α, IL-1β, IL-6 and MCP1 compared with *Ghsr*$^{f/f}$ ($p<0.05$), and there is no statistically difference in the sham control group. Some papers demonstrated that the pathology of depression in brain regions is from hippocampus to prefrontal cortex[47, 48]. In addition, *LysM-Cre*; *Ghsr*$^{f/f}$ promote the expression of BDNF than *Ghsr*$^{f/f}$ after CLP surgery at day8, and the BDNF data can also explain the *LysM-Cre*; *Ghsr*$^{f/f}$ mice reducing depression, stress and anxiety which is match with our previous behavior test data.

All these gene expression data suggested that the septic mouse model of *LysM-Cre*; *Ghsr*$^{f/f}$ mice reduced the pro-inflammation markers and improved the synapse plasticity through BDNF for decreasing the depression, stress, and anxiety.

Suppression of myeloid-specific GHS-R mediated the infiltration of macrophage in brain under CLP-induced sepsis

We used flow cytometry to separate the different cell groups in brain tissue and analyzed data by using FlowJo software. (**Fig. 5 A**) We drafted the flow chart to present how we separate cells, and the flow graph showed the details of cell separation. We referred to several papers about the gating strategy. (**Fig. 5 B**) To be more specific, many papers indicated that CD45 and CD11b are the markers for separating the myeloid cells[26], and Tmem119 is the unique marker for the microglia[25]. Also, Tmem119 can be utilized to separate the microglia and non-microglia myeloid cells. Additionally, microglia have two different states, one named resting microglia, and the other one named activated microglia. In the healthy brain, microglia exist as a "resting" state, and after a variety of stimulation, the resting microglia will be activated and release toxic cytokines and these activated microglia work as cytotoxic[49]. Some papers cited that CD11b+ CD45 intermitted Tmem119+ labeled as resting microglia, and CD11b+ CD45high Tmem119+ marked as activated microglia[24]. Furthermore, we used Ly6G and F4/80 to separate infiltrated monocytes, neutrophils, and macrophages. Additionally, CD86 and CD206 can separate the M1-like macrophage and M2-like macrophage from infiltrated macrophage in the brain[26]. (**Fig. 5 C**) In the flow analyzed data, we found that the cell ratio of resting microglia and activated microglia are no difference between *LysM-Cre*; *Ghsr*$^{f/f}$ and *Ghsr*$^{f/f}$ under

CLP treatment at day1. Also, the microglia data of flow cytometry is matched with immunofluorescence images' data that myeloid cell GHS-R knockout does not modulate the microglia under CLP-induced sepsis. The interesting thing is that we found that the neutrophils are increasing crucially in CLP groups compared with sham control groups ($p<0.05$). In normal conditions, neutrophils will have an associative increase in the cell number or cell ratio during sepsis[50]. It is well-known that neutrophils are the important innate immune cells during sepsis, which can secret inflammatory cytokines and have a phagocytosis function to eliminate the invading pathogens[51]. However, some papers demonstrated that sepsis could cause neutrophil dysfunctions which lead to organ failure[52]. Apart from that, we also found that the cell ratio of monocytes was also increasing dramatically in CLP groups compared with the sham control groups ($p<0.05$). It is no surprise that monocytes can increase in CLP-induced sepsis since monocytes play important roles in anti-infection[53]. However, we also found that M1-like infiltrated macrophage tends to decrease the cell ratio in *LysM-Cre*; $Ghsr^{f/f}$ compared with $Ghsr^{f/f}$ in CLP group ($P=0.13$) by using CD86 markers. In addition, the M2-like infiltrated macrophage tends to increase the cell ratio in *LysM-Cre*; $Ghsr^{f/f}$ compared with $Ghsr^{f/f}$ in CLP group ($P=0.08$) by using CD206 marker. Also, the M1/M2 like macrophage ratio showed a significant difference between *LysM-Cre*; $Ghsr^{f/f}$ and $Ghsr^{f/f}$ in the CLP group ($P<0.05$). There is no significant difference in sham control groups about the above separated myeloid cells. These data indicated that myeloid cell GHS-R knockout promotes the anti-inflammatory polarization of macrophage under CLP treatment at day1.

Suppression of myeloid-specific GHS-R promotes macrophage polarization through IS2/PI3K/AKT/mTOR and NF-κB cell signaling pathways.

To determine the regulated mechanism in GHS-R myeloid cells under endotoxic environment. We isolated the bone marrow derived macrophage (BMDM) to study the effect of GHS-R in macrophages, and to mimic sepsis-caused inflammation, we used 500ng/ml LPS solution to treat the BMDM[54]. Moreover, we did Western Blot (WB) to test the protein expression to reveal the cell signaling. Recent research showed that ablation of GHS-R is related to the insulin receptor substrate 2 expression[54]. (**Fig. 6**) Additionally, IRS2 represents the first nodes in the insulin signaling with the downstream nodes being phosphoinositide 3-kinase (PI3K) and protein kinase B (PKB/Akt) [55, 56]. Therefore, we detected the protein expression of IRS2, PI3K, and AKT, and found there are significantly reduced protein expressions in *LysM-Cre*; $Ghsr^{f/f}$ compared with $Ghsr^{f/f}$ in the LPS group ($P<0.05$). To be more specific, we did the phospho-AKT and total AKT with ImageJ analysis, and as well as the phospho-PI3K and total PI3K. In addition, some researchers reported that it is the known pathway that AKT can activate the mTOR and this cell signaling pathway is known as the PI3K/AKT/mTOR pathway in the autophagy and apoptosis[57, 58]. Thus, to investigate the expression of mTOR protein expression, we processed the phosphor-mTOR and total mTOR and found the p-mTOR/mTOR has crucially decreased in the *LysM-Cre*; $Ghsr^{f/f}$ comparing with $Ghsr^{f/f}$ in LPS group ($P<0.05$). Additionally, it is well-known that p65 is also named as NF-κB, and it can also work as the downstream of PI3K/AKT cell signaling pathways[59]. Thus, we test the phospho-p65 and total p65 protein expression (within the nuclear), and the data showed that there are significantly difference between *LysM-Cre*; $Ghsr^{f/f}$ and $Ghsr^{f/f}$ in LPS group ($P<0.05$), and p-p65/p65 ratio is reducing dramatically in *LysM-Cre*; $Ghsr^{f/f}$. Several papers demonstrated that PI3K/AKT/ NF-κB can activate the M1-like macrophage polarization and proliferation[60]. So, it can explain why

the M1-like infiltrated macrophage are decreasing in *LysM-Cre*; *Ghsr*$^{f/f}$ after CLP-induced sepsis in brain from flow cytometry data, since we ablation of the GHS-R expression on Macrophage and inactive the IS2/PI3K/AKT/mTOR and NF-κB cell signaling pathways to inhibit the M1-like macrophage polarization and activation. Furthermore, NLR family pyrin domain containing 3 (NLRP3) and caspase-1 are the downstream of the p65 and play critical roles in the innate immune system[61]. Therefore, to determine the caspase-1 whether been affected by the PI3K/AKT/ NF-κB cell signaling pathways as downstream, we also test the protein expression of caspase-1 and found that caspase-1 expression is also low in *LysM-Cre*; *Ghsr*$^{f/f}$ than *Ghsr*$^{f/f}$ after LPS treatment ($P<0.05$). Also, caspase-1 is the upstream and activation of IL-1β, and caspase-1 works as a scissor to cut the pro- IL-1β to release IL-1β as pro-inflammatory cytokines[62]. Furthermore, it has been reported that p38 mitogen-activated protein kinases (MAPKs) respond to the inflammatory cytokines such as IL-1β and are involved in cell apoptosis and autophagy[63]. So, we also tested the phospho-p38 and total p38 and found the p-p38/p38 ratio is decreasing in *LysM-Cre*; *Ghsr*$^{f/f}$ group after the LPS group ($P<0.05$).

In summary, (**Fig. 7**) myeloid GHS-R can play important roles in the activation and polarization of macrophages by IRS2-PI3K-AKT-mTOR and P65 signaling cascades.

CONCLUSION

These results indicated that the deletion of myeloid cell GHS-R knockout plays important roles in reducing the anxiety, stress, and depression from the OFT and TST behavior test. Additionally, the ablation of GHS-R in myeloid cells reduces the pro-inflammatory cytokines and promotes macrophage polarization from the qPCR and flow cytometry data. Also, we found that BDNF expression was increasing after CLP-induced sepsis at day8, and it can explain the behavior test that can reduce anxiety, stress, and depression. (**Fig. 7**) Furthermore, GHS-R plays important roles in the activation and polarization of infiltrated macrophages by IRS2/PI3K/mTOR/NF- κB cell signaling pathways from the Western Blot data. Our research is to reveal the potential GHS-R cell signaling pathway, and we get further understanding of the GHS-R associated molecular pathological mechanism in sepsis. More importantly, deletion of GHS-R can be potentially translated to clinical therapeutic application in the future.

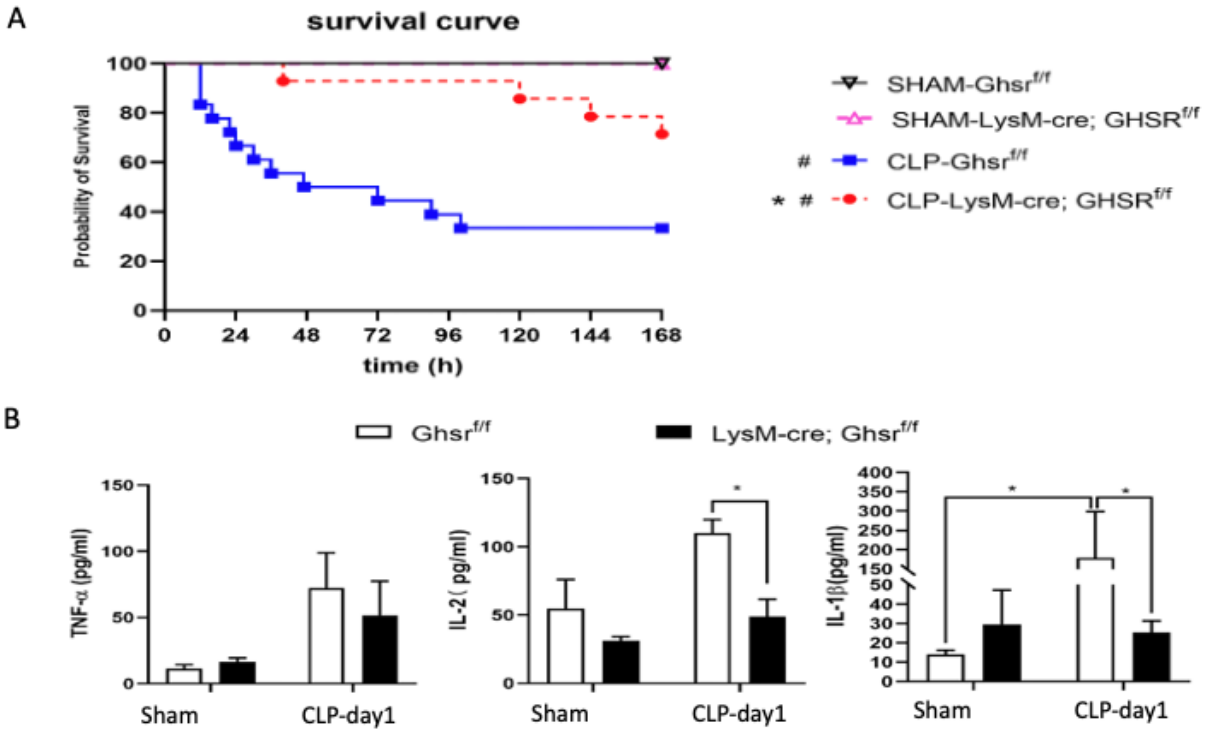

Figure 1. (A) Survival after CLP-induced sepsis. Kaplan-Meier survival curves of mice after CLP-induced sepsis. Sham group (n=14), *CLP-Ghsr*$^{f/f}$ under group (n=18), *CLP-LysM-Cre*; *Ghsr*$^{f/f}$ (n=14). # $P < 0.001$ significantly different from sham-operated group and *$P < 0.05$ significantly different from *CLP-Ghsr*$^{f/f}$ group, both determined by the log-rank test. (B) The cytokines in serum (Sham group n=4, CLP group n=6). Data are expressed as mean ± SEM. TNF-α, IL-2, IL-1β statistical analysis using two-way ANOVA followed by the Tukey's multiple comparisons test and* $P<0.05$.

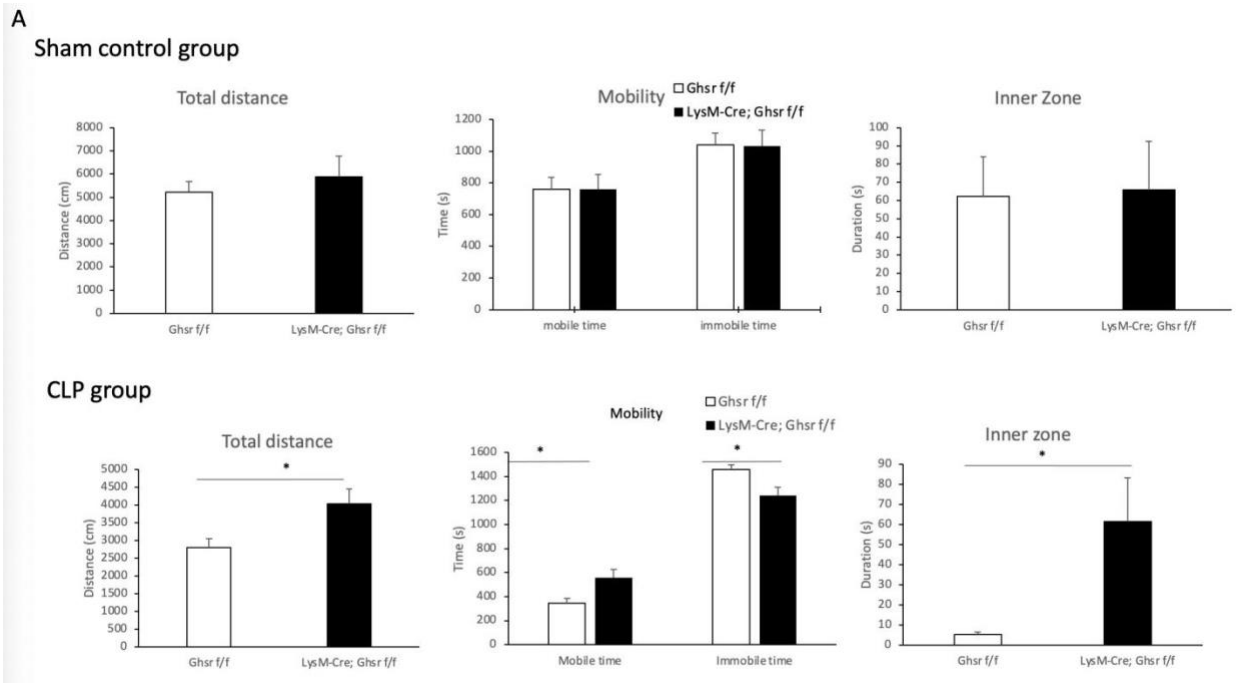

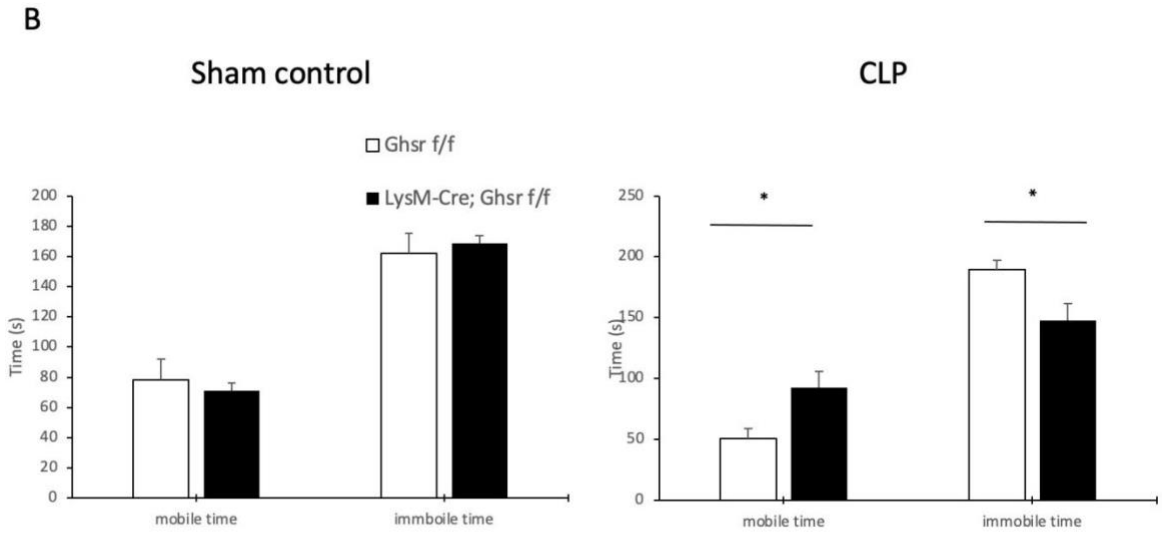

Figure 2. (A) Open field test (OFT) of 6-month old RD fed (n=4 *Ghsr*$^{f/f}$ mice and n=4 *LysM-cre; Ghsr*$^{f/f}$ mice) sham control group mice. *Ghsr*$^{f/f}$ vs. *LysM-cre; Ghsr*$^{f/f}$. All data are presented as means ± SEM. OFT of 6-month old RD fed (n=5 *Ghsr*$^{f/f}$ mice and n=8 *LysM-cre; Ghsr*$^{f/f}$ mice) group mice at day3. *p<0.05, *Ghsr*$^{f/f}$ vs. *LysM-cre; Ghsr*$^{f/f}$.All data are presented as means ± SEM. (B) Tail Suspension test of 6-month old RD fed (n=4 *Ghsr*$^{f/f}$ mice and n=4 *LysM-cre; Ghsr*$^{f/f}$ mice) Sham control group mice. *Ghsr*$^{f/f}$ vs. *LysM-cre; Ghsr*$^{f/f}$. All data are presented as means ± SEM.

TST of 6-month old RD fed (n=5 *Ghsr*$^{f/f}$ mice and n=8 *LysM-cre; Ghsr*$^{f/f}$ mice) CLP surgery group mice at day5. *p<0.05, *Ghsr*$^{f/f}$ vs. *LysM-cre; Ghsr*$^{f/f}$. All data are presented as means ± SEM.

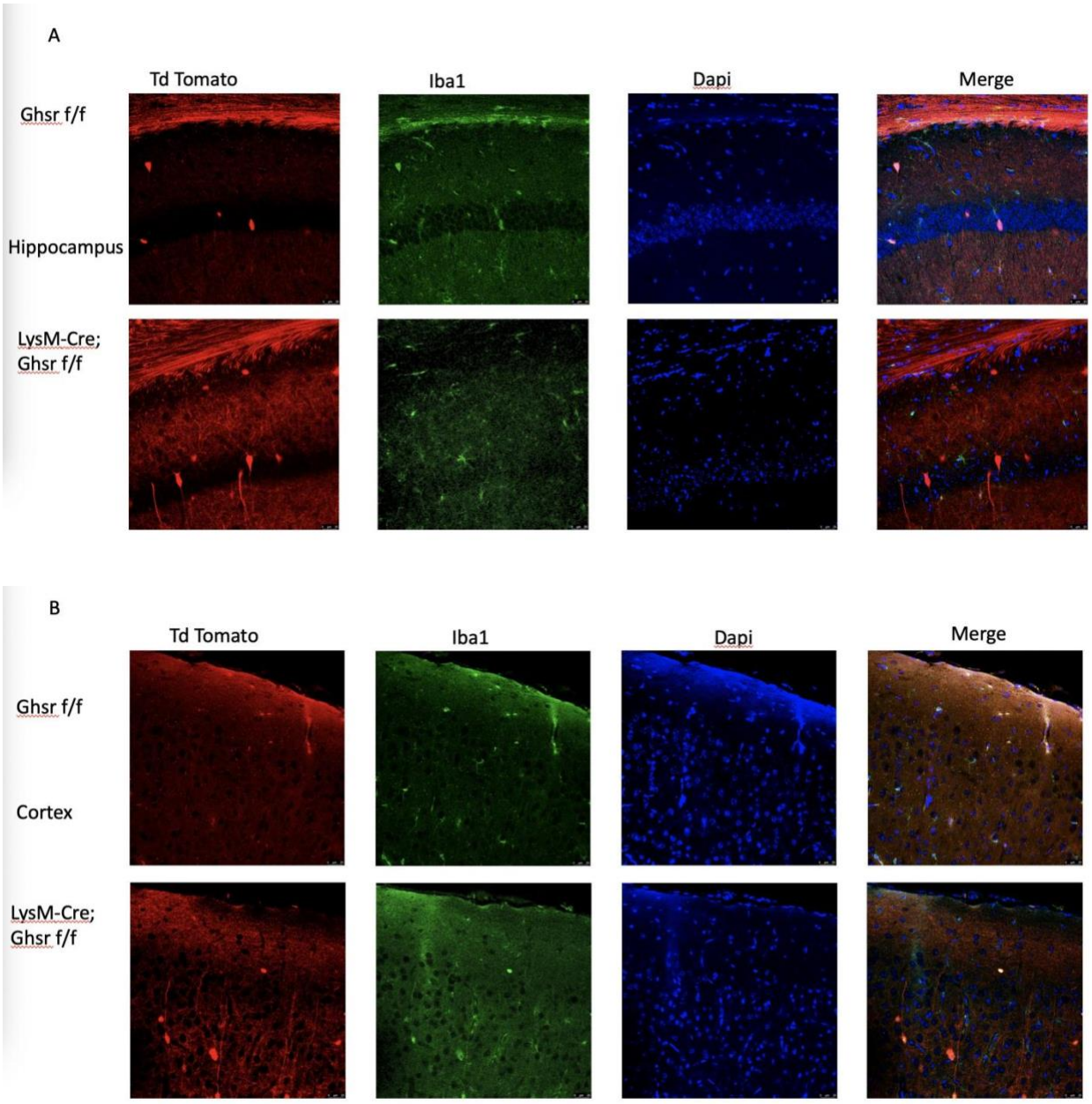

Figure 3. Immunofluorescence of brain tissues including hippocampus, cortex.

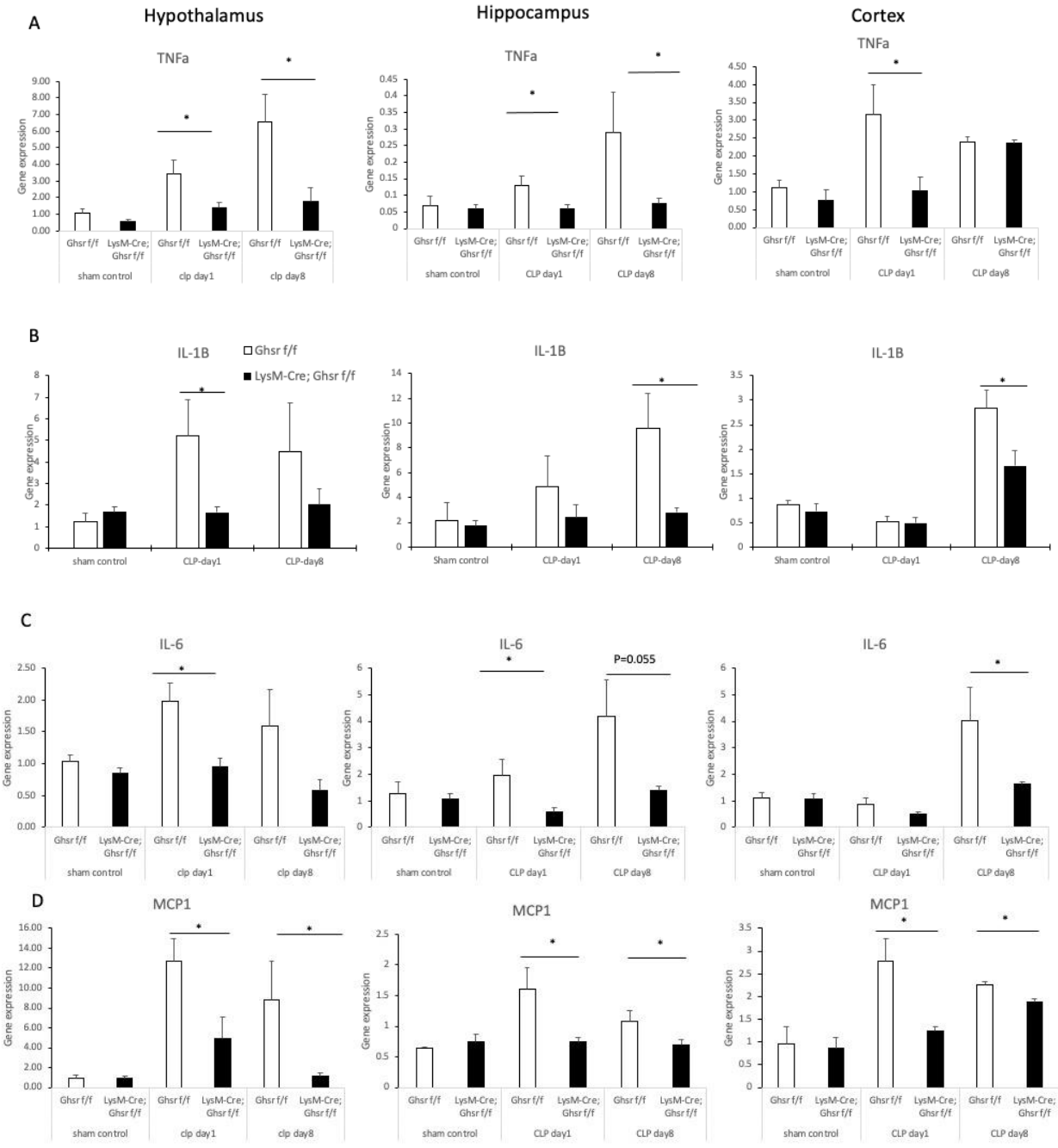
A
Hypothalamus
Hippocampus
Cortex
TNFa
Gene expression
Ghsr f/f
LysM-Cre; Ghsr f/f
sham control
clp day1
clp day8
CLP day1
CLP day8
B
IL-1B
Ghsr f/f
LysM-Cre; Ghsr f/f
sham control
CLP-day1
CLP-day8
Sham control
C
IL-6
P=0.055
D
MCP1

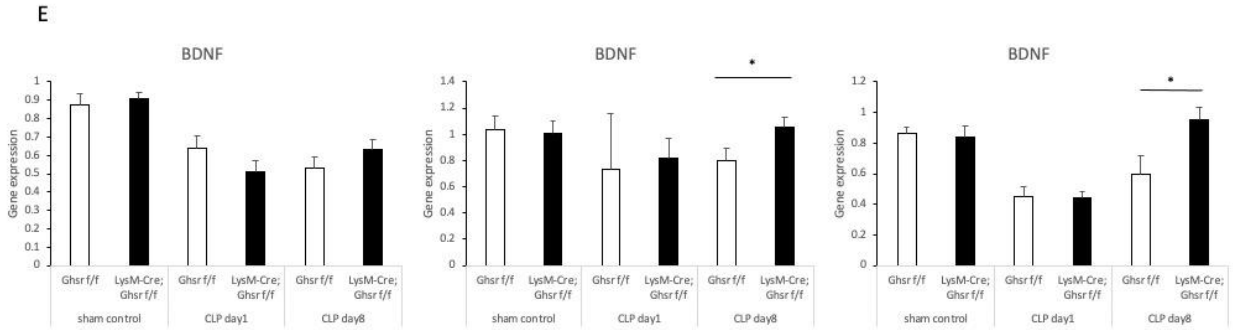

Figure 4. Pro-inflammatory cytokines including TNF- α, IL-1β, IL-6, MCP1 and BDNF in the hypothalamus, cortex and hippocampus. CLP RD mice were sacrificed at the age of 4-6 months. Sham control RD mice were sacrificed at the age of 6 months. Gene expression of inflammatory cytokines in the hypothalamus, cortex and hippocampus. LysM-cre;Ghsr f/f was decreased under both acute phase and recovery phase of sepsis. n=4 *Ghsr*$^{f/f}$ mice and n=4 *LysM-cre; Ghsr*$^{f/f}$ mice in sham control group. n=5 *Ghsr*$^{f/f}$ mice and n=6 *LysM-cre; Ghsr*$^{f/f}$ mice in CLP day1 acute phase of sepsis group. n=4 *Ghsr*$^{f/f}$ mice and n=4 *LysM-cre; Ghsr*$^{f/f}$ mice in sham control group. n=6 *Ghsr*$^{f/f}$ mice and n=6 *LysM-cre; Ghsr*$^{f/f}$ mice in CLP day8 recovery phase of sepsis group *p<0.05, **p<0.001, *Ghsr f/f* vs. *LyzM-cre; Ghsr f/f*. All data are presented as means ± SEM.

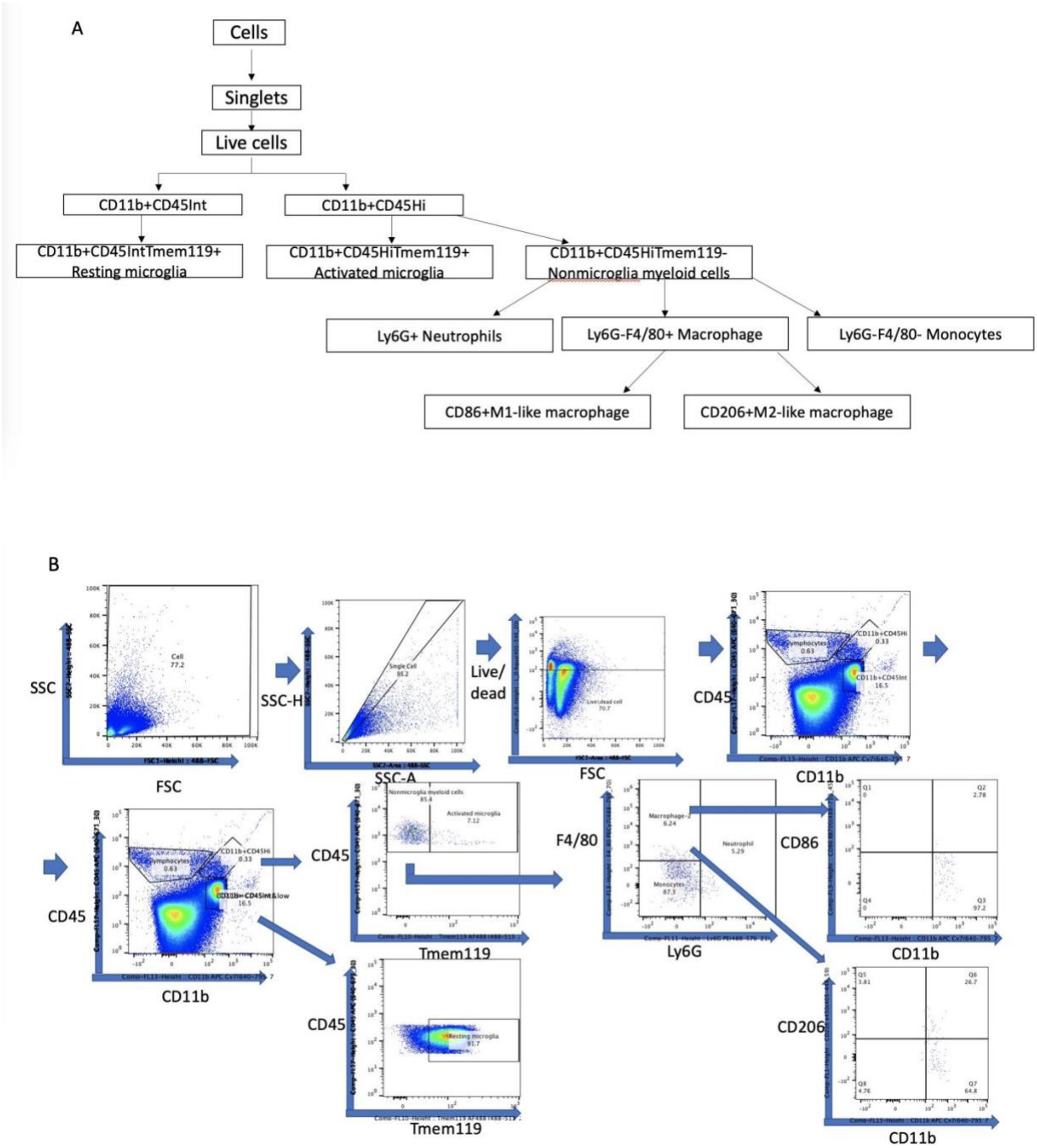
A
Cells
Singlets
Live cells
CD11b+CD45Int
CD11b+CD45Hi
CD11b+CD45IntTmem119+
Resting microglia
CD11b+CD45HiTmem119+
Activated microglia
CD11b+CD45HiTmem119-
Nonmicroglia myeloid cells
Ly6G+ Neutrophils
Ly6G-F4/80+ Macrophage
Ly6G-F4/80- Monocytes
CD86+M1-like macrophage
CD206+M2-like macrophage
B
SSC
FSC
SSC-H
SSC-A
Live/
dead
FSC
CD45
CD11b
CD45
CD11b
CD45
Tmem119
F4/80
Ly6G
CD86
CD11b
CD45
Tmem119
CD206
CD11b

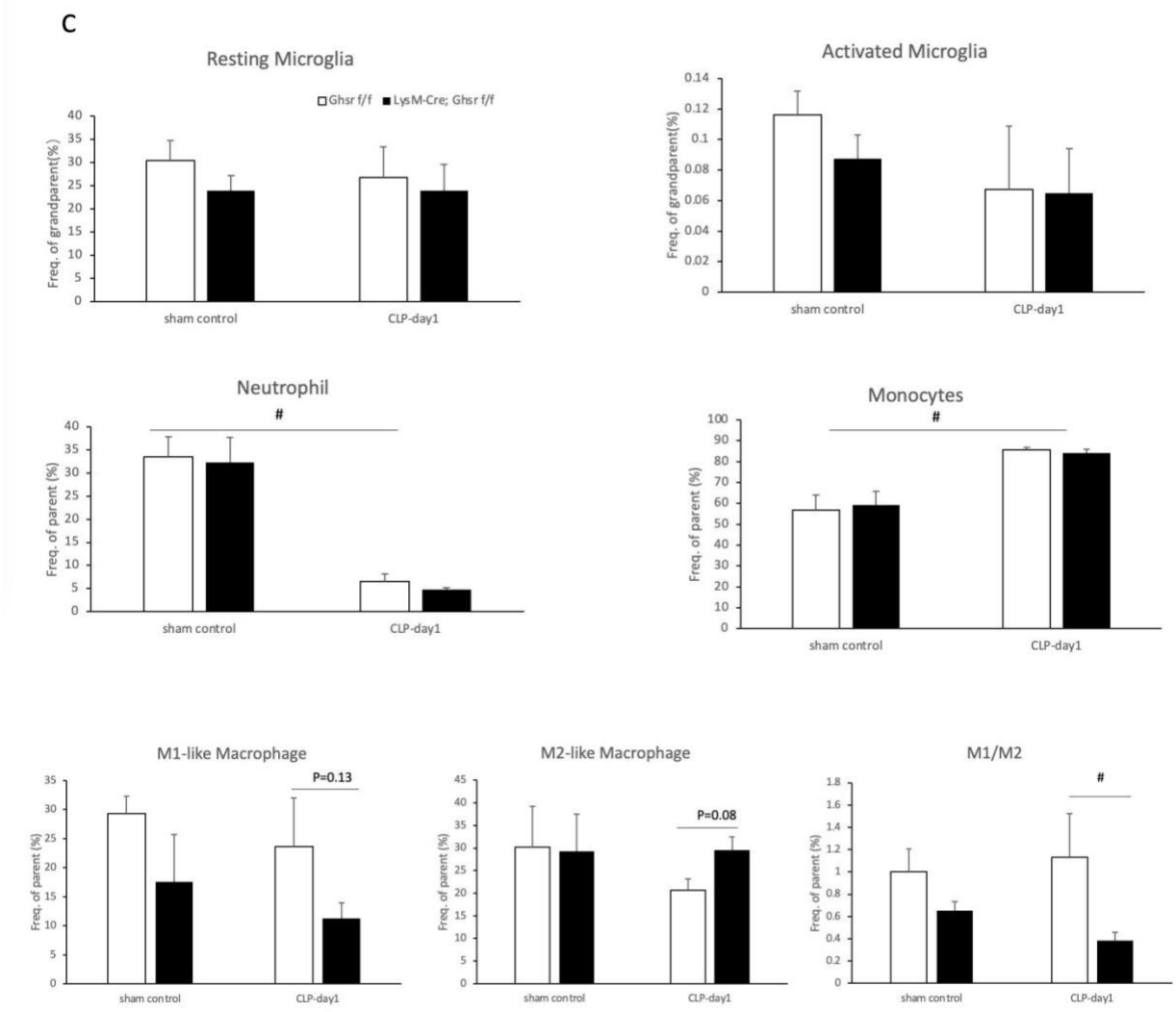

Figure 5. (A) Gating Strategy flow chat for brain immune cells. (B) Representative flow picture of brain after CLP treatment at day1 and sham control groups. (C) Representative histograms. Data are expressed as mean ± SEM. Statistical analysis using two-way ANOVA followed by the Tukey's multiple comparisons test, * P<0.05, ** P<0.01, *** P<0.001. The y-axis of C is frequency in parent as cell ratio.

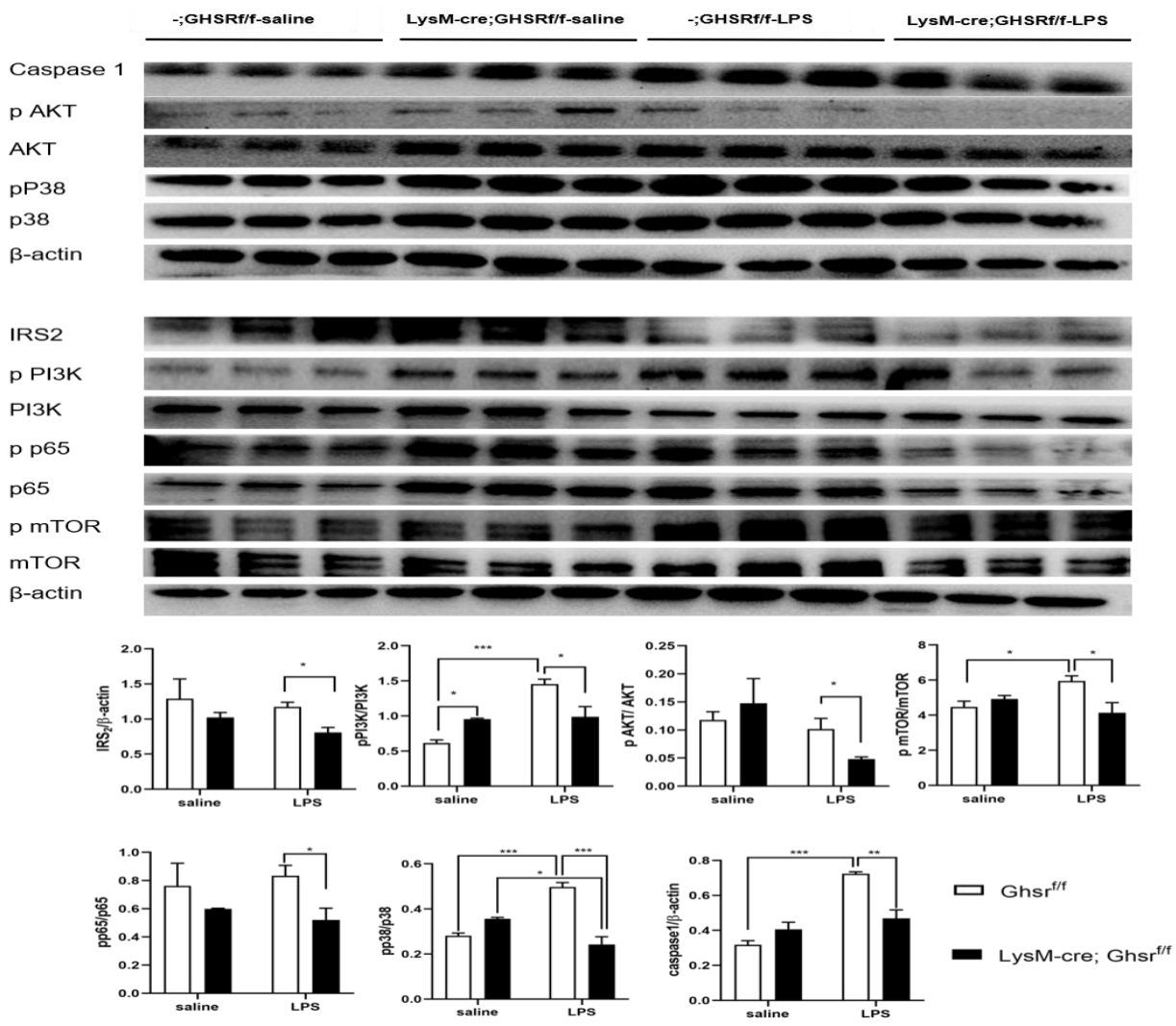

Figure 6. The immune blot for the protein expression of BMDM involved in IRS2-PI3K-AKT-mTOR and P65 signaling pathways. BMDM are treated with saline or 500ng/ml LPS solution for 6 hours. Data are expressed in mean ± SEM. Statistical analysis using two-way ANOVA, * P<0.05, ** P<0.01, *** P<0.001.

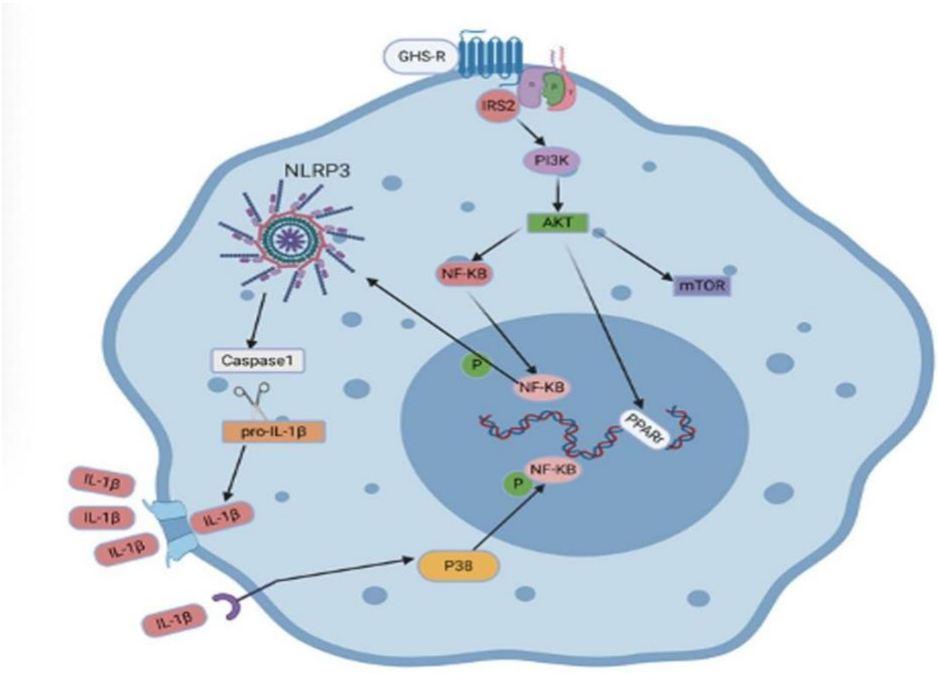

Figure 7. Potential cell signaling pathway

Table 1
Sequence of primers used in the qPCR analysis

mRNA	Forward	Reverse
TNF-α	GCCCACGTCGTAGCAAAC	GCAGCCTTGTCCCTTGAA
IL-1β	TGTTCTTTGAAGTTGACGGACCC	TCATCTCGGAGCCTGTAGTGC
IL-6	CCAGAGATACAAAGAAATGATGG	ACTCCAGAAGACCAGAGGAAAT
MCP1	CTTCTGGGCCTGCTGTTCA	CCAGCCTACTCATTGGGATCA
BDNF	ATAGTAACGAACAGGATGG	GCTCAGTCATGGGAGTCC

Table 2
Antibodies used to stain cells

Antigen	Conjugate	Dilution
Live Dead	Aqua	1:1000
CD45	APC	1:100
Ly6G	PE	1:100
CD11b	APCcy7	1:80
Tmem119	Alex Flour 488	1:40
F4/80	PE-cy7	1:200
CD206	Eflour450	1:40
CD86	BB700	1:100

REFERENCES

1. Steinert, R.E., et al., *Ghrelin, CCK, GLP-1, and PYY(3-36): Secretory Controls and Physiological Roles in Eating and Glycemia in Health, Obesity, and After RYGB.* Physiol Rev, 2017. **97**(1): p. 411-463.

2. Laviano, A., et al., *The growth hormone secretagogue receptor (Ghs-R).* Curr Pharm Des, 2012. **18**(31): p. 4749-54.

3. Furness, J.B., et al., *Investigation of the presence of ghrelin in the central nervous system of the rat and mouse.* Neuroscience, 2011. **193**: p. 1-9.

4. Schaeffer, M., et al., *Rapid sensing of circulating ghrelin by hypothalamic appetite-modifying neurons.* Proc Natl Acad Sci U S A, 2013. **110**(4): p. 1512-7.

5. Fang, C., et al., *Ghrelin Signaling in Immunometabolism and Inflamm-Aging.* Adv Exp Med Biol, 2018. **1090**: p. 165-182.

6. Zhang, C.S., et al., *The Correlation Between Circulating Ghrelin and Insulin Resistance in Obesity: A Meta-Analysis.* Front Physiol, 2018. **9**: p. 1308.

7. Porporato, P.E., et al., *Acylated and unacylated ghrelin impair skeletal muscle atrophy in mice.* J Clin Invest, 2013. **123**(2): p. 611-22.

8. Andrews, Z.B., *The extra-hypothalamic actions of ghrelin on neuronal function.* Trends Neurosci, 2011. **34**(1): p. 31-40.

9. Sun, Y., S. Ahmed, and R.G. Smith, *Deletion of ghrelin impairs neither growth nor appetite.* Mol Cell Biol, 2003. **23**(22): p. 7973-81.

10. Ma, X., et al., *Ghrelin receptor regulates HFCS-induced adipose inflammation and insulin resistance.* Nutr Diabetes, 2013. **3**(12): p. e99.

11. Dolin, H.H., et al., *Characterization of Pathogenic Sepsis Etiologies and Patient Profiles: A Novel Approach to Triage and Treatment.* Microbiol Insights, 2019. **12**: p. 1178636118825081.

12. Cecconi, M., et al., *Sepsis and septic shock.* Lancet, 2018. **392**(10141): p. 75-87.

13. Atterton, B., et al., *Sepsis Associated Delirium.* Medicina (Kaunas), 2020. **56**(5).

14. Evans, T., *Diagnosis and management of sepsis.* Clin Med (Lond), 2018. **18**(2): p. 146-149.

15. Ruiz, S., et al., *Sepsis modeling in mice: ligation length is a major severity factor in cecal ligation and puncture.* Intensive Care Medicine Experimental, 2016. **4**(1): p. 22.

16. Lewis, A.J., C.W. Seymour, and M.R. Rosengart, *Current Murine Models of Sepsis.* Surg Infect (Larchmt), 2016. **17**(4): p. 385-93.

17. Palpagama, T.H., et al., *The Role of Microglia and Astrocytes in Huntington's Disease.* Frontiers in Molecular Neuroscience, 2019. **12**(258).

18. Avau, B., et al., *Ghrelin signaling in the gut, its physiological properties, and therapeutic potential.* Neurogastroenterology & Motility, 2013. **25**(9): p. 720-732.

19. Lee, J.H., et al., *Neuronal Deletion of Ghrelin Receptor Almost Completely Prevents Diet-Induced Obesity.* Diabetes, 2016. **65**(8): p. 2169-78.

20. Sun, Y., J.M. Garcia, and R.G. Smith, *Ghrelin and growth hormone secretagogue receptor expression in mice during aging.* Endocrinology, 2007. **148**(3): p. 1323-9.

21. Seibenhener, M.L. and M.C. Wooten, *Use of the Open Field Maze to measure locomotor and anxiety-like behavior in mice.* J Vis Exp, 2015(96): p. e52434.

22. Can, A., et al., *The tail suspension test.* J Vis Exp, 2012(59): p. e3769.

23. Steelman, A.J. and J. Li, *Astrocyte galectin-9 potentiates microglial TNF secretion.* J Neuroinflammation, 2014. **11**: p. 144.

24. Choi, J.Y., et al., *Indispensable Role of CX3CR1+ Dendritic Cells in Regulation of Virus-Induced Neuroinflammation Through Rapid Development of Antiviral Immunity in Peripheral Lymphoid Tissues.* Frontiers in Immunology, 2019. **10**(1467).

25. Bennett, M.L., et al., *New tools for studying microglia in the mouse and human CNS.* Proceedings of the National Academy of Sciences, 2016. **113**(12): p. E1738-E1746.

26. Xu, X., et al., *Anti-inflammatory and immunomodulatory mechanisms of atorvastatin in a murine model of traumatic brain injury.* J Neuroinflammation, 2017. **14**(1): p. 167.

27. Choleris, E., et al., *A detailed ethological analysis of the mouse open field test: effects of diazepam, chlordiazepoxide and an extremely low frequency pulsed magnetic field.* Neurosci Biobehav Rev, 2001. **25**(3): p. 235-60.

28. Miller, B.H., et al., *Phenotypic characterization of a genetically diverse panel of mice for behavioral despair and anxiety.* PLoS One, 2010. **5**(12): p. e14458.

29. *Dedication*, in *Photobiomodulation in the Brain*, M.R. Hamblin and Y.-Y. Huang, Editors. 2019, Academic Press. p. v.

30. Salehpour, F., et al., *Chapter 14 - Photobiomodulation for depression in animal models*, in *Photobiomodulation in the Brain*, M.R. Hamblin and Y.-Y. Huang, Editors. 2019, Academic Press. p. 189-205.

31. Filiano, A.J., S.P. Gadani, and J. Kipnis, *Interactions of innate and adaptive immunity in brain development and function.* Brain Res, 2015. **1617**: p. 18-27.

32. González Ibanez, F., et al., *Immunofluorescence Staining Using IBA1 and TMEM119 for Microglial Density, Morphology and Peripheral Myeloid Cell Infiltration Analysis in Mouse Brain.* J Vis Exp, 2019(152).

33. Xu, Y., et al., *Quantifying blood-brain-barrier leakage using a combination of evans blue and high molecular weight FITC-Dextran.* J Neurosci Methods, 2019. **325**: p. 108349.

34. Shaner, N.C., et al., *Improved monomeric red, orange and yellow fluorescent proteins derived from Discosoma sp. red fluorescent protein.* Nat Biotechnol, 2004. **22**(12): p. 1567-72.

35. Musetti, R. and S.V. Buxa, *DAPI and Confocal Laser-Scanning Microscopy for In Vivo Imaging of Phytoplasmas.* Methods Mol Biol, 2019. **1875**: p. 301-306.

36. Orthgiess, J., et al., *Neurons exhibit Lyz2 promoter activity in vivo: Implications for using LysM-Cre mice in myeloid cell research.* European Journal of Immunology, 2016. **46**(6): p. 1529-1532.

37. Toscano, M.G., D. Ganea, and A.M. Gamero, *Cecal ligation puncture procedure.* J Vis Exp, 2011(51).

38. Chiswick, E.L., et al., *Acute-Phase Deaths from Murine Polymicrobial Sepsis Are Characterized by Innate Immune Suppression Rather Than Exhaustion.* J Immunol, 2015. **195**(8): p. 3793-802.

39. Parameswaran, N. and S. Patial, *Tumor necrosis factor-α signaling in macrophages.* Crit Rev Eukaryot Gene Expr, 2010. **20**(2): p. 87-103.

40. Swardfager, W., et al., *A meta-analysis of cytokines in Alzheimer's disease.* Biol Psychiatry, 2010. **68**(10): p. 930-41.

41. Lopez-Castejon, G. and D. Brough, *Understanding the mechanism of IL-1β secretion.* Cytokine Growth Factor Rev, 2011. **22**(4): p. 189-95.

42. Song, J., et al., *Diagnostic and prognostic value of interleukin-6, pentraxin 3, and procalcitonin levels among sepsis and septic shock patients: a prospective controlled study according to the Sepsis-3 definitions.* BMC Infectious Diseases, 2019. **19**(1): p. 968.

43. Ting, E.Y., A.C. Yang, and S.J. Tsai, *Role of Interleukin-6 in Depressive Disorder.* Int J Mol Sci, 2020. **21**(6).

44. Deshmane, S.L., et al., *Monocyte chemoattractant protein-1 (MCP-1): an overview.* J Interferon Cytokine Res, 2009. **29**(6): p. 313-26.

45. Miranda, M., et al., *Brain-Derived Neurotrophic Factor: A Key Molecule for Memory in the Healthy and the Pathological Brain.* Frontiers in Cellular Neuroscience, 2019. **13**(363).

46. Dwivedi, Y., *Brain-derived neurotrophic factor: role in depression and suicide.* Neuropsychiatr Dis Treat, 2009. **5**: p. 433-49.

47. Liu, W., et al., *The Role of Neural Plasticity in Depression: From Hippocampus to Prefrontal Cortex.* Neural Plast, 2017. **2017**: p. 6871089.

48. Gujral, S., et al., *Exercise effects on depression: Possible neural mechanisms.* Gen Hosp Psychiatry, 2017. **49**: p. 2-10.

49. Cherry, J.D., J.A. Olschowka, and M.K. O'Banion, *Are "Resting" Microglia More "M2"?* Frontiers in Immunology, 2014. **5**(594).

50. Shen, X.F., et al., *Neutrophil dysregulation during sepsis: an overview and update.* J Cell Mol Med, 2017. **21**(9): p. 1687-1697.

51. Kovach, M.A. and T.J. Standiford, *The function of neutrophils in sepsis.* Current Opinion in Infectious Diseases, 2012. **25**(3): p. 321-327.

52. Zhang, F., et al., *Neutrophil Dysfunction in Sepsis.* Chin Med J (Engl), 2016. **129**(22): p. 2741-2744.

53. Venet, F. and G. Monneret, *Advances in the understanding and treatment of sepsis-induced immunosuppression.* Nat Rev Nephrol, 2018. **14**(2): p. 121-137.

54. Zughaier, S.M., H.C. Ryley, and S.K. Jackson, *Lipopolysaccharide (LPS) from Burkholderia cepacia is more active than LPS from Pseudomonas aeruginosa and Stenotrophomonas maltophilia in stimulating tumor necrosis factor alpha from human monocytes.* Infect Immun, 1999. **67**(3): p. 1505-7.

55. Mao, N., et al., *Oncogenic ERG Represses PI3K Signaling through Downregulation of IRS2.* Cancer Res, 2020. **80**(7): p. 1428-1437.

56. Yang, L., et al., *miR-431 regulates granulosa cell function through the IRS2/PI3K/AKT signaling pathway.* J Reprod Dev, 2020. **66**(3): p. 231-239.

57. Heras-Sandoval, D., et al., *The role of PI3K/AKT/mTOR pathway in the modulation of autophagy and the clearance of protein aggregates in neurodegeneration.* Cellular Signalling, 2014. **26**(12): p. 2694-2701.

58. Xu, F., et al., *RETRACTED ARTICLE: Roles of the PI3K/AKT/mTOR signalling pathways in neurodegenerative diseases and tumours.* Cell & Bioscience, 2020. **10**(1): p. 54.

59. Xu, Y., et al., *Irgm1 is required for the inflammatory function of M1 macrophage in early experimental autoimmune encephalomyelitis.* J Leukoc Biol, 2017. **101**(2): p. 507-517.

60. Linton, M.F., J.J. Moslehi, and V.R. Babaev, *Akt Signaling in Macrophage Polarization, Survival, and Atherosclerosis.* Int J Mol Sci, 2019. **20**(11).

61. Kelley, N., et al., *The NLRP3 Inflammasome: An Overview of Mechanisms of Activation and Regulation.* Int J Mol Sci, 2019. **20**(13).

62. Galliher-Beckley, A.J., et al., *Caspase-1 activation and mature interleukin-1β release are uncoupled events in monocytes.* World J Biol Chem, 2013. **4**(2): p. 30-4.

63. Cosgrove, B.D., et al., *Rejuvenation of the muscle stem cell population restores strength to injured aged muscles.* Nat Med, 2014. **20**(3): p. 255-64.